

# ELECTROMAGNETIC FIELD CHARACTERISTICS OF WATER FILM SENSOR IN INTELLIGENT TRANSPORT SYSTEM

Yasumitsu MIYAZAKI and Ken TANAKA  
 Department of Information and Computer Sciences  
 Toyohashi University of Technology  
 Tempaku-cho, Toyohashi, 441-8580, Japan  
 E-mail miyazaki@emlab.tutics.tut.ac.jp

## 1. Introduction

In the recent years, transportation using vehicles plays a very important role and contributes considerably to the development of present social economic system. But, as the transport systems develop, we have increased traffic congestion and accidents, environmental pollution due to exhaust, and these lead to serious problems to the society. In order to solve the above problems, it becomes necessary for the construction of Intelligent Transport System(ITS)[1] by considering the human, roads and vehicles as a single combined unit. In the field of ITS, research and development have been accelerated to accomplish danger warning provisions and assistance to driving.

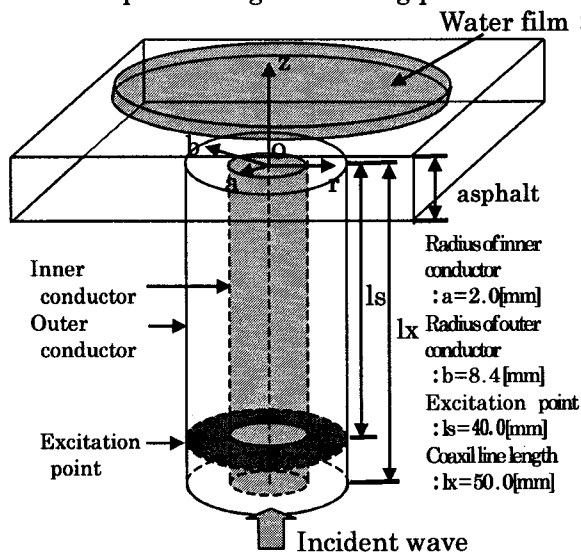


Fig.1 Water film sensor

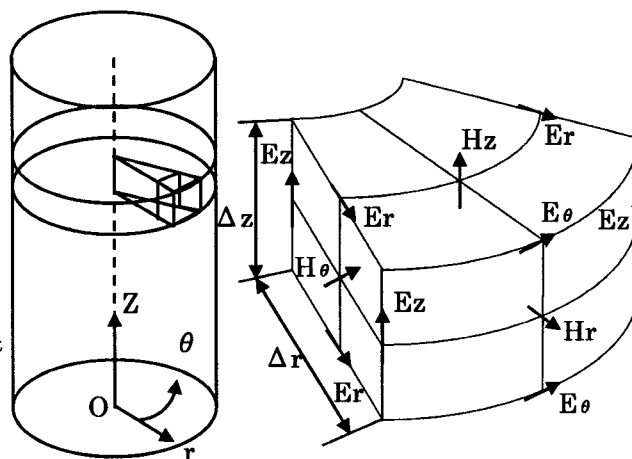


Fig.2 Spatial arrangement of electromagnetic field and analysis region

For the realization of automatic, safe and comfortable driving Advanced Cruise-Assist Highway System(AHS) has been developed.

It is important to obtain information on road conditions and estimation of distance between moving vehicles for accident prevention. As a means to solve these problems, the AHS is given increasing attention in the recent years. Even though various sensors have been developed for the detection of road condition, the problems of developing low-cost electromagnetic wave type sensors that can be used irrespective of various weather conditions have yet to be solved completely. Therefore it is important to give attention to develop a non-contact type water film sensors which are expected to be more efficient and low-cost and can be applied to the present transport system. The water film sensor is laid underground, and microwaves are allowed to propagate through the asphalt tube and made incident on the water film formed over

the road surface. The thickness of the film is estimated from the reflection characteristics. We employed coaxial transmission lines in the water film sensor and it has the advantages such as low-cost and easy to make connections. For numerical simulations of the sensor type explained above, we employed Finite Difference Time Domain (FDTD) method with cylindrical coordinate system. This method can deal with both steady-state and transient conditions of the sensing process.

We study Electromagnetic field characteristic of water film sensor in AHS, and it is final purpose to try high variable and more efficient sensor

## 2. Analysis method

### 2.1 Finite Difference Time Domain (FDTD)with cylindrical coordinate system

Various numerical simulation techniques are employed in the electromagnetic analysis such as finite element method and boundary element method. In our study, we adopted FDTD method, with which it is possible to simulate the steady state and transient characteristics of open-type and inhomogeneous media efficiently. As shown in Fig.4, the components of electromagnetic fields can be represented in the cylindrical coordinate system [2,3]. In the present model shown in figure, since we have symmetry in the axial direction, the derivative with respect to  $\theta$  is zero, the problem is solved in two-dimension as given by the eqs.(1)~(3). The corresponding difference equations are given by eqs.(4)~(6). The constants appeared in eqs.(4)~(6) are given in eqs.(7)~(10)

$$\begin{aligned} \frac{\partial E_r}{\partial z} - \frac{\partial E_z}{\partial r} &= -\mu \frac{\partial H_\theta}{\partial t} & (1) \quad H_\theta^{n+\frac{1}{2}}(i+\frac{1}{2}, k+\frac{1}{2}) &= H_\theta^{n-\frac{1}{2}}(i+\frac{1}{2}, k+\frac{1}{2}) \\ -\frac{\partial H_\theta}{\partial z} &= \sigma E_r + \varepsilon \frac{\partial E_r}{\partial t} & (2) \quad &+ \left\{ \frac{1}{\Delta z} \left( E_r^n(i+\frac{1}{2}, k+1) - E_r^n(i+\frac{1}{2}, k) \right) \right. \\ \frac{1}{r} \frac{\partial}{\partial r} (r H_\theta) &= \sigma E_z + \varepsilon \frac{\partial E_z}{\partial t} & (3) \quad &\left. - \frac{1}{\Delta r} \left( E_z^n(i+1, k+\frac{1}{2}) - E_z^n(i, k+\frac{1}{2}) \right) \right\} \quad (6) \end{aligned}$$

$$E_r^n(i+\frac{1}{2}, k) = A_r \cdot E_r^{n-1}(i+\frac{1}{2}, k) \quad A_r = \frac{2\varepsilon(i+\frac{1}{2}, k) - \sigma(i+\frac{1}{2}, k)\Delta t}{2\varepsilon(i+\frac{1}{2}, k) + \sigma(i+\frac{1}{2}, k)\Delta t} \quad (7)$$

$$-B_r \cdot \frac{1}{\Delta z} \left( H_\theta^{n-\frac{1}{2}}(i+\frac{1}{2}, k+\frac{1}{2}) - H_\theta^{n-\frac{1}{2}}(i+\frac{1}{2}, k-\frac{1}{2}) \right) \quad B_r = \frac{2dt}{2\varepsilon(i+\frac{1}{2}, k) + \sigma(i+\frac{1}{2}, k)\Delta t} \quad (8)$$

$$E_z^n(i, k+\frac{1}{2}) = A_z \cdot E_z^{n-1}(i, k+\frac{1}{2}) \quad A_z = \frac{2\varepsilon(i, k+\frac{1}{2}) - \sigma(i, k+\frac{1}{2})\Delta t}{2\varepsilon(i, k+\frac{1}{2}) + \sigma(i, k+\frac{1}{2})\Delta t} \quad (9)$$

$$+ B_z \cdot \frac{1}{r(i, k+\frac{1}{2}) \cdot \Delta r} \left( r(i+\frac{1}{2}) \cdot H_\theta^{n-\frac{1}{2}}(i+1, k+\frac{1}{2}) - r(i-\frac{1}{2}) \cdot H_\theta^{n-\frac{1}{2}}(i-\frac{1}{2}, k+\frac{1}{2}) \right) \quad B_z = \frac{2\Delta t}{2\varepsilon(i, k+\frac{1}{2}) + \sigma(i, k+\frac{1}{2})\Delta t} \quad (10)$$

### 2.2 Simulation parameter

The frequency range used in the simulation is 1-6[GHz]. Simulations are carried out with cell size in the radial direction set to be less than 1/10 of the wavelength in water film, and we used first order absorbing boundary conditions. The stability condition of the FDTD method with cylindrical coordinate system is given by the following equation.

$$V \max \cdot \Delta t \leq \left( \frac{1}{\Delta r^2} + \frac{1}{\Delta z^2} \right)^{-\frac{1}{2}} \quad (11)$$

### 3. Results and Discussion

#### 3.1 Reflection and return loss of two-layer type loss dielectric

We compare our simulation results on water film sensor with the other approximate analysis and experimental results reported for a similar model by Ganchev [4,5]. Fig.6 shows the change in the reflection and return loss as a function of  $d_1$ . The parameters used for the simulations are shown in Fig.5 and  $\Gamma$  denotes the reflection coefficient and RL denotes the reflection and return loss.

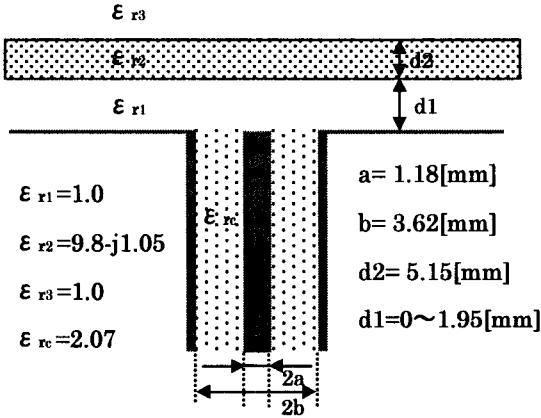


Fig.5 Two-layer type lossy dielectric model

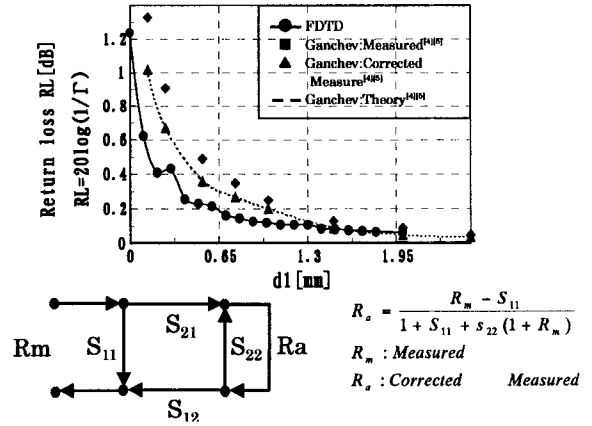


Fig.6 Compare of reflection and return loss with Two layer type loss dielectric

#### 4.2 Reflection and return loss due to thin water film

To further understand the fundamental characteristics of the water film sensor, we performed similar calculations without the asphalt. The model is shown in Fig.7. The electric field on the open part of the water film sensor plays an important role. Fig.8 and 9 shows the variation of reflection and return loss as a function of frequency and thickness of water film respectively, and the other parameters are shown in the figure. The electric field distribution in the open part of the sensor is shown in Fig.10-13, and the direction of electric fields is compared. In the graphs we have shown only a part of the sensor centered on the water film. The amplitude and direction of the electric fields at points A, B and C are listed in Table 1.

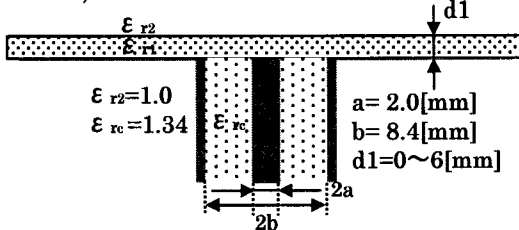


Fig.7 Water film sensor

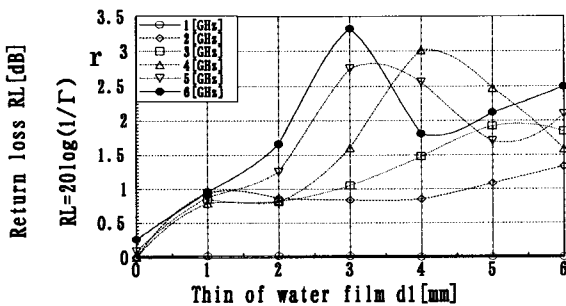


Fig. 8. Reflection and return loss as a function of Thickness

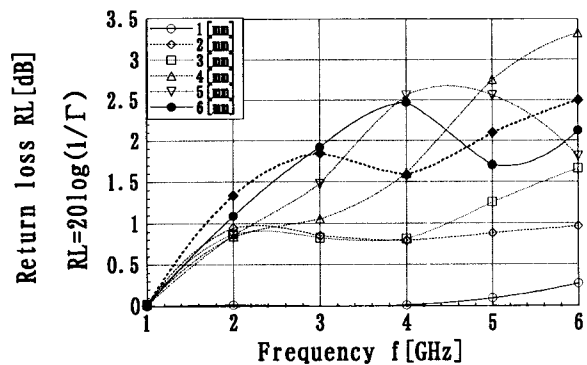


Fig.9 Reflection and return loss of the sensor

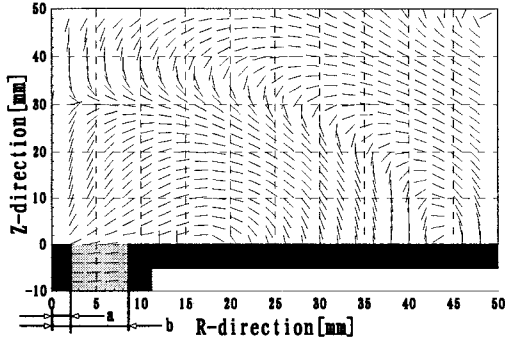


Fig.10 Electric field distribution(240[ps])  
f=6[GHz] a=2[mm],b=8.4[mm]

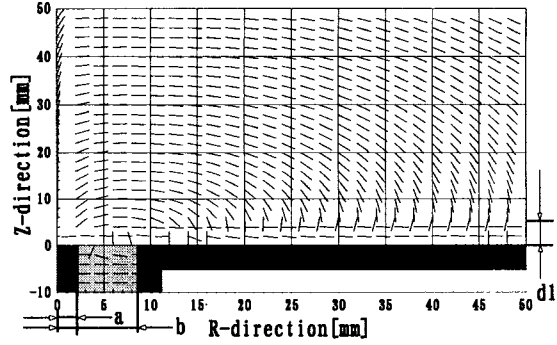


Fig.12 Electric field distribution(240[ps])  
f=6[GHz] a=2[mm],b=8.4[mm],d1=5[mm]

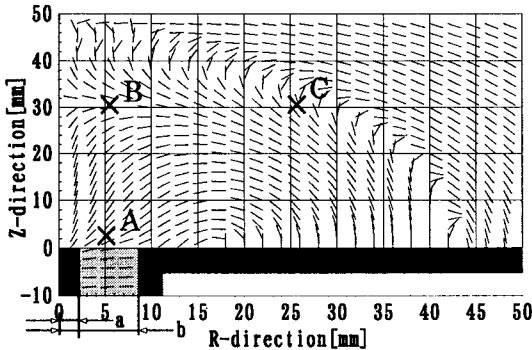


Fig.11 Electric field distribution(320[ps])  
f=6[GHz] a=2[mm],b=8.4[mm]

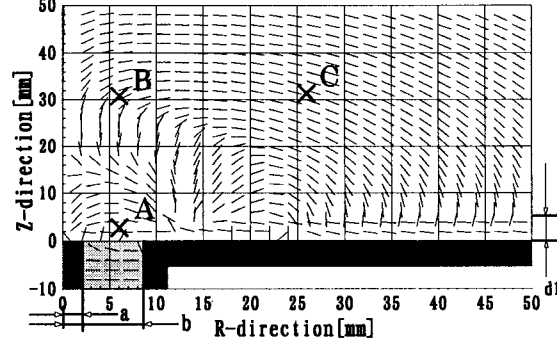


Fig.13 Electric field distribution(320[ps])  
f=6[GHz] a=2[mm],b=8.4[mm],d1=5[mm]

Table 1 Amplitude of electric field in A, B and C points

	A (6,2)	B (6,30)	C (26,30)
Open (Fig.11)	69.83[v/m]	1.83[v/m]	2.69[v/m]
d1=5[mm] of water film (Fig.13)	17.19[v/m]	0.80[v/m]	0.07[v/m]

A point r=6 z=2[mm], B point r=6 z=30[mm], C point r=26 z=30 [mm]

## 5. Conclusions and Future Directions

We have presented the simulation results on water film sensor and shown the electromagnetic characteristics. We have studied the dependence of sensing characteristics with respect to the sensor parameters. In the future, we planned to carry out simulations to study the accuracy and error due to the FDTD method with cylindrical coordinates. Also simulations have to be carried out by varying other parameters of the sensor for optimum design of the water film sensor.

### Acknowledgements

The authors would like to acknowledge the assistance, support, and efforts of Ishizu, Nakamura, Katsumi as well as the other members of the ITS research center of Furukawa Electric Co.Ltd.

### Reference

- [1]Japan society of traffic engineers: "Intelligent transport system"1997
- [2]K. Takahashi and Y. Miyazaki : IEE of Japan, vol.118-C, no.1, pp.93-98, 1998
- [3]Y. Chen, R. Mittra and P. Harms: IEEE Trans. on Microwave Theory Tech.. Vol.44, No.6,pp.832-839,1996.
- [4]S. I. Ganchev and N. Qaddoumi: IEEE Trans. on Instrum. Meas., Vol.44, No.6, pp.1023-1029,1995
- [5]S. Bakhtiari, S. I. Ganchev and R. Zoughi: IEEE Trans. on Microwave Theory Tech.. Vol.42, No.7, pp.1261-1267, 1994.